Tidal and Residual Currents in the Northern North Sea: Observations

Holger Klein, Wolfgang Lange and Ekkehard Mittelstaedt

UDC 551.466.78:551.466.75

Summary

One-month current and water-level time series from the northern North Sea are analyzed with regard to residual flows, volume transports, and tidal constituents. The data originate from the **NORA** and **MOVENS** field programs (along 59° N, July/August 1990 and roughly 62° N, September/October 1986 respectively). With regard to the residual flows, the results generally confirm the known circulation pattern of the northern North Sea. Differences between these and other investigations are due to the great short and long-term variability of the current systems. The main objective of this paper, however, is to describe tides and tidal streams. Firstly, we relate the tidal streams along 59° N to the spring and neap high waters at Aberdeen; secondly, up to 17 tidal constituents are determined by means of harmonic analysis.

Gezeiten und Restströme in der nördlichen Nordsee: Beobachtungen (Zusammenfassung)

Einmonatige Strömungs- und Wasserstandszeitserien aus der nördlichen Nordsee werden hinsichtlich der Restströme, Volumentransporte und Gezeiten analysiert. Die Daten stammen aus den beiden Meßprogrammen **NORA** entlang 59° N (Juli/August 1990) und **MOVENS** entlang ca. 62° N (September/Oktober 1986). Die berechneten Restströme entsprechen dem bekannten generellen Zirkulationsmuster in der nördlichen Nordsee. Im einzelnen auftretende Abweichungen zu anderen Untersuchungen haben ihre Ursache in der starken Variabilität der Restströme in diesem Seegebiet. Hauptanliegen dieser Arbeit ist die Darstellung der Gezeiten und Gezeitenströme. Im ersten Schritt werden die Gezeitenströme entlang 59° N zu den Spring- und Nipp-Gezeiten in Aberdeen in Beziehung gesetzt. In einem zweiten Schritt werden mit Hilfe der harmonischen Analyse die Koeffizienten von bis zu 17 Partialtiden berechnet.

1 Introduction

The water exchange across the northern boundary of the North Sea is dominated by the in- and outflow through the Norwegian Trench. The trench is the main link between the shallow North Sea and the deep Atlantic Ocean. The transition zone between the shelf and the deep sea is also the northern boundary of several numerical North Sea circulation models. A main problem in modelling is posed by the great length of the open northern boundary of the North Sea, together with the great variability of volume transports in several time scales. Most of these models use only the M_2 tidal elevation. Higher tidal harmonics, however, are also important for North Sea dynamics and are generated on the shelf itself (cf. Delhez and Martin [1992]). Besides discussing tidal and residual currents, we therefore also determine tidal constituents which could be used to improve the boundary information for circulation models. The results of two field experiments are discussed below.

Methods:

During the **NORA** experiment (**Nor**d **Ra**nd, northern boundary), 8 current meter moorings, each equipped with 3–5 Aanderaa RCM4/5 current meters, were deployed along 59° N between 2° W and 4° 45' E (N1–N8 in Fig. 1). The moorings were maintained for about one month from 15–17 July until 18–21 August, 1990.

The **MOVENS** moorings (**Mo**del **Ve**rification **N**orth **S**ea) were deployed between 6 and 8 September 1986, and recovered between 15 and 19 October 1986. The MOVENS moorings (M7–M10 in Fig. 1) were

deployed along 61° 51' N between 1° 30' E and 4° 10' E. For all NORA and MOVENS instruments, the sampling interval was 10 minutes, except for the deepest MOVENS instruments which were acoustic Neil-Brown current meters with a sampling interval of 1 minute.

The N1 to N5 NORA moorings and the M8 and M9 MOVENS moorings were additionally equipped with Aanderaa water level recorders. Deployment positions, sampling depths, and soundings are given in Table 1. All instruments returned full records.

Table 1

Deployment statistics

Id	Position laditude	longitude	water depth	sampling depths current meters					WLR
			m	m	m	m	m	m	m
			"NORA" July/August 1990						
N1	59° 0.16' N	1° 59.85' W	80	24,	46,	66,	78	–	77
N2	59° 0.10' N	1° 0.30' W	129	22,	63,	100,	127	–	126
N3	59° 0.19' N	0° 0.57' W	138	25,	66,	109,	–	–	135
N4	59° 0.02' N	1° 0.31' E	125	22,	63,	96,	123	–	122
N5	59° 0.23' N	2° 0.43' E	116	13,	21,	62,	114	–	113
N6	58° 59.95' N	3° 29.94' E	210	21,	73,	124,	156,	208	–
N7	59° 0.10' N	4° 10.11' E	295	16,	67,	256,	293	–	–
N8	58° 59.90' N	4° 44.88' E	280	16,	68,	149,	251,	278	–
			"MOVENS" September/October 1986						
M6	60° 28.90' N	3° 31.60' E	312	117,	189,	247,	304	–	–
M7	61° 50.37' N	2° 2.87' E	375	70,	120,	225,	288,	365	–
M8	61° 50.57' N	1° 29.79' E	355	90,	163,	226,	286,	348,	236
M9	61° 50.95' N	3° 0.19' E	413	60,	130,	240,	300,	403,	280
M10	61° 51.71' N	4° 9.55' E	210	55,	75,	126,	176,	205	–

Id = mooring identifier, WLR = water level recorder

2 Residual currents and volume transports

This section describes volume transports and residual currents at the NORA and MOVENS sections. To eliminate inertial and tidal motions, periods shorter than 24.48 hours are removed using a Gaussian low-pass filter. Volume transports were calculated from the low-passed meridional velocity components, averaged over the length of the respective time series (see Tables 2 and 3). The box contours (Fig.3) are placed right between the current meters (horizontal lines) and mooring positions (vertical lines), respectively.

2.1 The NORA section (July/August 1990)

The water exchange across the NORA section is dominated by the northward outflow of the Norwegian Coastal Current (NCC) and the southward inflow of Atlantic Water (AW) at the western edge of the Norwegian Trench. In the upper layer, the NCC is the continuation of the Baltic Current, a narrow wedge of low salinity water close to the coast, and a wider section of mixed North Sea water. The day to day variability of the NCC and AW transports is greater than their mean values (Otto et al.[1990]). The boundary between the NCC and the inflow of AW is characterized by great mesoscale variability which manifests itself in mesoscale meanders and eddies (Ikeda et al.[1989], Johannessen et al.[1989]). Between 58.5°N and 59° N the continuous AW inflow is blocked by a submarine ridge (cf. Furnes et al. [1986]). Through a combination of topographic steering and Ekman transport, most of the AW inflow makes a cyclonic turn and flows back northwards with the NCC (Turrell [1992a]).

Table 2

Summary statistics of low-frequency currents – NORA section

	instrument depth	$\overline{u}$	$\overline{u'u'}$	$\overline{v}$	$\overline{v'v'}$	v	SF	dir.	k_E	k_M
	m	cm/s	cm²/s²	cm/s	cm²/s²	cm/s	%	°	cm²/s²	
N1	24	–6.9	23.6	–6.5	49.5	9.5	27	227	36.5	45.3
	46	–6.5	15.4	–3.4	36.8	7.4	35	242	26.3	27.3
	66	–3.0	11.4	–4.3	45.4	5.3	21	215	28.4	13.9
	78	–1.5	8.3	–2.1	17.9	2.6	17	215	13.1	3.5
N2	22	1.4	24.2	–0.7	25.7	1.6	7	117	24.9	1.2
	63	1.5	24.8	–1.0	33.2	1.8	9	124	29.0	1.6
	100	0.4	11.2	–0.2	38.6	0.5	3	127	24.9	0.1
	127	–0.5	16.2	–0.5	23.0	0.7	5	228	19.6	0.2
N3	25	0.9	11.4	–0.8	28.6	1.3	5	132	20.0	0.8
	66	2.3	7.2	–0.5	26.7	2.3	17	102	16.9	2.8
	109	2.3	10.2	–0.1	28.7	2.3	18	92	19.5	2.6
N4	22	8.6	40.2	–1.0	17.1	8.6	41	96	28.6	37.2
	63	3.6	40.1	–0.0	7.8	3.6	22	90	24.0	6.6
	96	1.8	21.0	–0.8	6.7	2.0	15	113	13.8	1.9
	123	1.0	10.4	–0.1	3.8	1.0	12	94	7.1	0.5
N5	21	15.0	133.1	–1.5	50.3	15.1	49	96	91.7	113.9
	62	9.8	72.4	–1.0	31.9	9.8	50	96	52.2	48.5
	114	4.5	48.2	–0.4	3.7	4.5	47	95	25.9	10.0
N6	21	–0.6	65.1	–2.4	54.7	2.5	11	194	59.9	3.1
	73	1.0	75.2	–6.1	37.3	6.2	37	171	56.2	19.3
	124	1.4	24.2	–4.8	14.9	5.0	47	164	19.5	12.6
	156	1.3	29.3	–5.2	7.2	5.4	61	166	18.3	14.6
	208	2.2	14.5	–3.2	8.2	3.9	53	146	11.3	7.7
N7	15	–0.8	247.0	8.4	129.5	8.5	26	354	185.8	35.8
	67	0.7	46.3	8.0	30.6	8.0	57	5	38.4	32.4
	256	0.6	11.2	8.2	19.9	8.2	69	4	15.5	33.4
	293	0.0	0.9	–0.5	1.3	0.5	8	175	1.1	0.1
N8	16	–5.6	78.7	10.0	126.0	11.5	41	331	102.3	66.3
	68	–0.8	14.0	2.4	33.2	2.5	28	342	23.6	3.1
	149	0.0	8.0	1.3	15.5	1.3	15	2	11.8	0.8
	251	0.9	8.8	1.1	16.9	1.5	18	38	12.9	1.1
	278	1.7	12.2	–1.2	3.6	2.0	39	125	7.9	2.1

$\overline{u}$, $\overline{v}$ = means of the zonal and meridional component of the current vector;
$\overline{u'u'}$, $\overline{v'v'}$ = zonal and meridional variances;
v = mean vector speed;
SF = stability factor: $(v/v_s) * 100$;
dir = mean direction;
k_E, k_M = eddy and mean kinetic energy

Table 3

Summary statistics of low-frequency currents – MOVENS section

	instrument depth	$\bar{u}$	$\overline{u'u'}$	$\bar{v}$	$\overline{v'v'}$	v	SF	dir.	k_E	k_M
	m	cm/s	cm²/s²	cm/s	cm²/s²	cm/s	%	°	cm²/s²	
M6	117	0.6	24.5	–4.0	74.6	4.1	32	171	49.5	8.3
	189	0.9	13.4	–2.6	53.7	2.7	27	162	33.5	3.8
	247	0.4	21.1	–1.9	29.7	1.9	23	167	25.4	1.9
	304	0.7	18.0	2.0	21.0	2.1	22	20	38.1	2.3
M7	70	–6.7	96.2	1.0	131.7	6.7	41	279	114.0	22.8
	120	–8.3	93.4	–1.1	82.9	8.3	55	262	88.2	34.9
	225	–6.2	57.4	4.1	98.9	7.4	53	303	78.1	27.5
	288	–5.5	45.0	4.7	89.9	7.3	54	310	67.4	26.4
	365	–6.1	53.9	5.4	88.7	8.2	59	312	71.3	33.3
M8	90	4.5	18.2	–8.6	46.7	9.7	78	153	32.4	47.0
	163	4.5	16.5	–7.0	44.9	8.3	75	148	30.7	34.7
	226	3.1	34.8	–5.7	36.3	6.5	69	151	35.5	21.5
	286	3.3	12.7	–4.8	38.5	5.8	62	145	25.6	17.0
	348	3.6	22.3	–2.4	41.9	4.3	46	123	32.1	9.2
M9	60	–0.5	37.1	–4.1	86.3	4.1	34	187	61.7	8.5
	130	–0.6	66.7	–4.0	44.7	4.0	38	189	55.7	8.1
	240	–0.7	33.4	–0.1	34.8	0.7	9	263	34.1	0.2
	300	–0.1	25.9	1.4	33.1	1.4	18	355	29.5	1.0
	403	–0.4	39.0	3.7	48.8	3.8	39	353	43.9	7.1
M10	55	–0.9	86.1	12.1	90.5	12.1	67	355	88.3	73.3
	75	1.1	31.0	7.5	45.6	7.5	65	8	38.3	28.5
	126	0.3	1.7	0.9	3.0	0.9	29	17	2.4	0.5
	205	0.0	13.3	1.7	29.3	1.7	22	1	21.3	1.5

$\bar{u}, \bar{v}$ = means of the zonal and meridional component of the current vector;
$\overline{u'u'}, \overline{v'v'}$ = zonal and meridional variances;
v = mean vector speed;
SF = stability factor: $(v/v_s) * 100$;
dir = mean direction;
k_E, k_M = eddy and mean kinetic energy

According to Svendsen et al. [1991], some AW enters the North Sea east of the Shetlands with great year to year variability. In addition, mixed Scottish coastal water and AW enter through the Orkney-Shetland channel southwards, known as the **F**air **I**sle **C**urrent (**FIC**). The FIC has a seasonal variability with volume transports of the order of 4×10^5 m³/s in the summer and 1.5×10^5 m³/s in the winter. At about 58° N, the FIC turns eastwards and – known as the Dooley Current – roughly follows the 100 m isobath towards the Norwegian Trench (Turrell et al. [1990]).

Figure 1 shows the vertically averaged, low-passed mean currents (vectors at the NORA and MOVENS positions, together with the general circulation pattern. The mean currents at each instrument are shown in Figure 2. In Figure 1, no account is taken of the data from the upper 30 metres of the water column. This is done to minimize the influence of the local wind. Moorings N6 to N8 were placed across the Norwegian trench. N7 lies in the center of the trench, close to the maximum depth of the NORA section. N6 and N7 lie on the western and eastern slope of the trench, respectively. As expected, we observe the outflow of the NCC at N7 and N8, and the inflow of AW at N6 at the western edge of the Norwegian Trench (see Fig. 3). The associated volume transports during NORA amounted to about 13×10^5 m³/s (NCC) and 6×10^5 m³/s (AW).

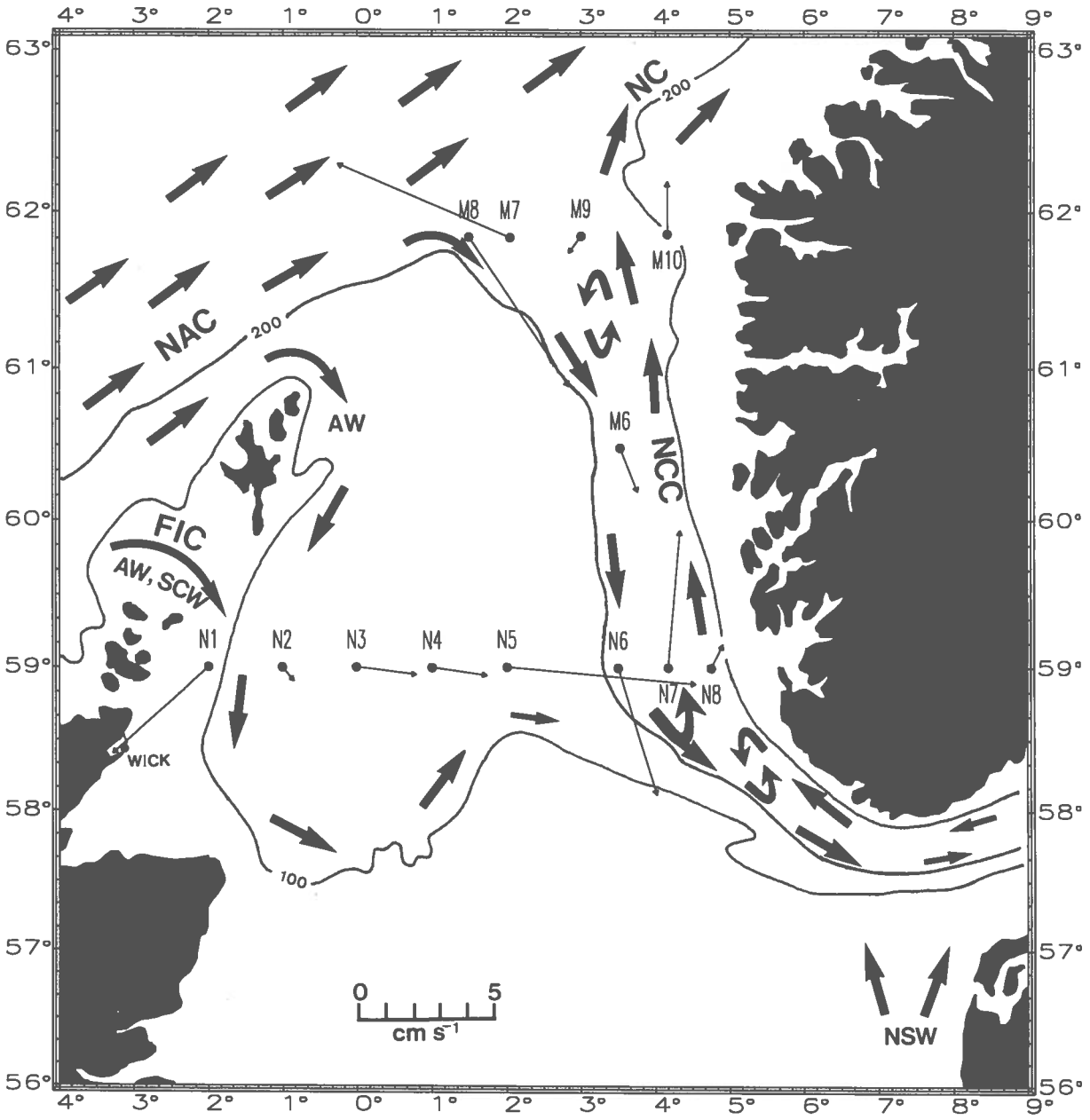

Fig. 1 Mooring positions and vertically (>30 m) averaged low-passed mean current vectors. The large scale circulation pattern is schematically outlined. NAC = North Atlantic Current, NC = Norwegian Current, NCC = Norwegian Coastal Current, FIC = Fair Isle Current. AW = Atlantic Water, SCW = Scottish Coastal Water.

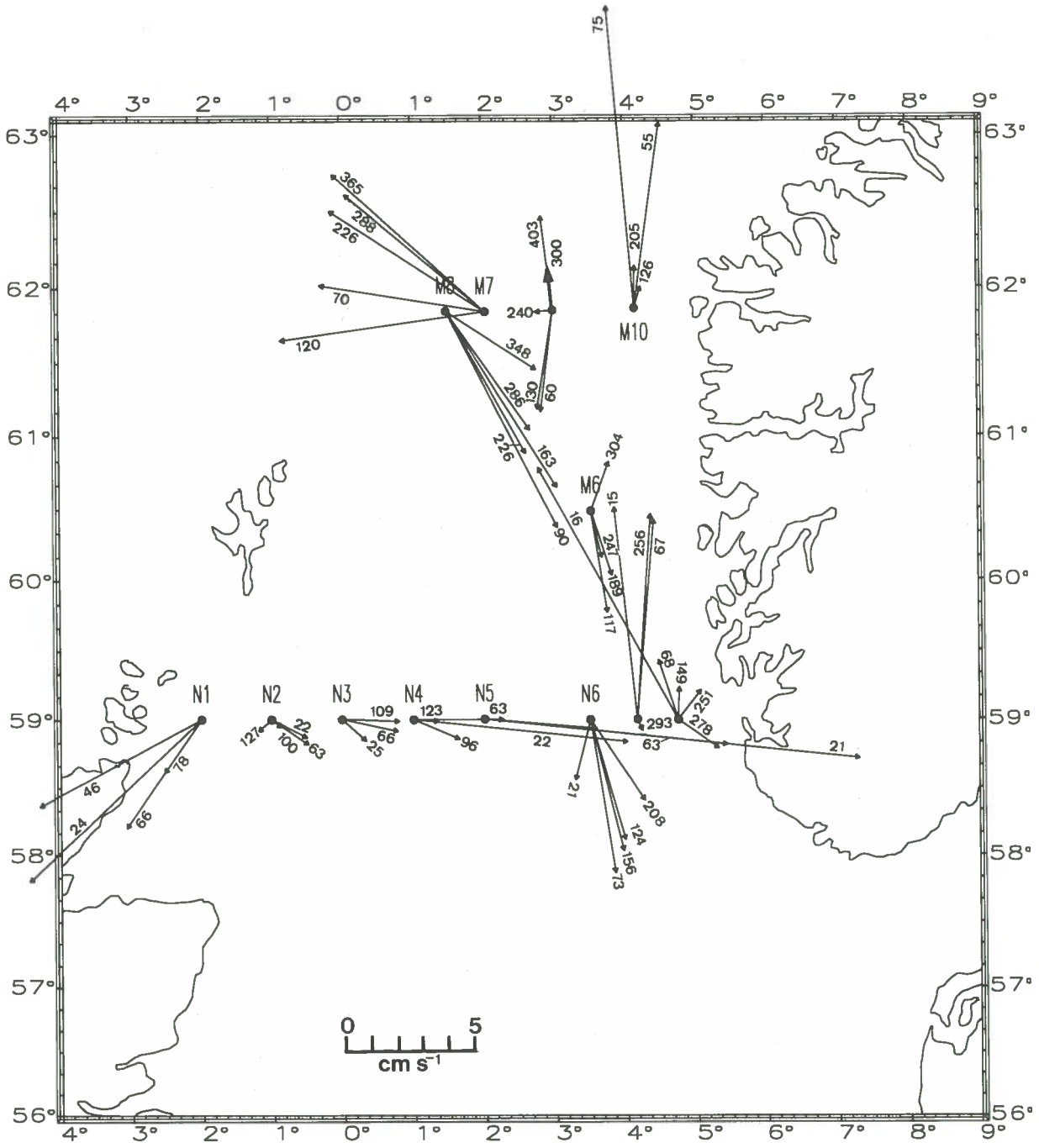

Fig. 2 Mean low-passed current vector for each current meter. The numbers at the vectors give the sampling depths in metres.

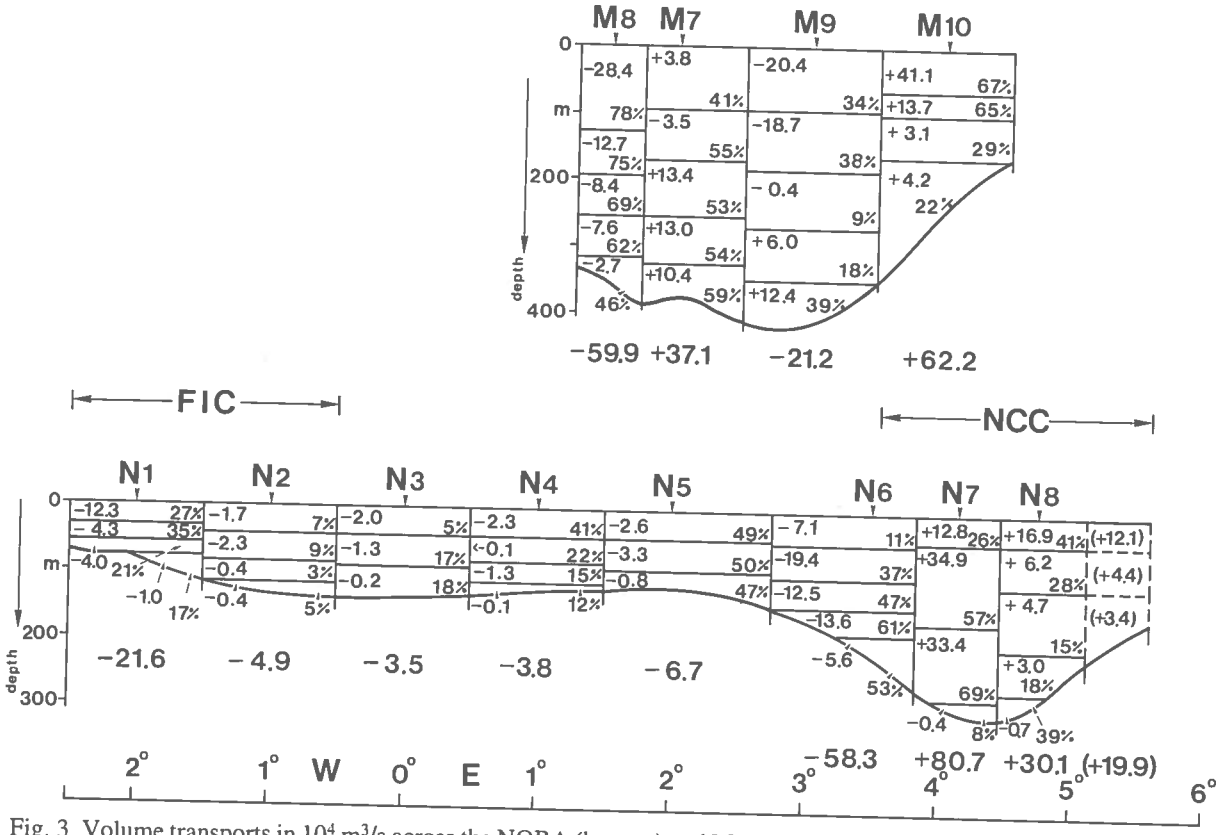

Fig. 3 Volume transports in 10^4 m^3/s across the NORA (bottom) and MOVENS section (top). Outflow (northward) positive and inflow (southward) negative. The numbers at the right side of each box give the stability of the current in percent. The broken boxes eastward of N8 give extrapolated volume transports between 5° 10' E and 5° 40' E. Total transport rates for each section segment are given under the bottom line.

The estimated total inflow between 2° 30' W and 2° 45' E (N1-N5) amounts only to 4×10^5 m^3/s (Fig. 3). The main contribution of about 2.6×10^5 m^3/s comes from the Fair Isle Current which is known to follow the 100 m isobath approximately (N1, N2). Turrell et al. [1990] estimated the Fair Isle inflow to be about 3×10^5 m^3/s – with great month to month variability, however. The strong eastward flow between N3 and N5 forms part of the northern edge of the topographically-guided Dooley Current.

Statistics of the low-passed NORA data are summarized in Table 2. The directional variability of the flow is expressed as a stability factor (*SF*), i. e. the ratio between mean vector speed v and mean scalar speed v_s in percent: $SF = (v/v_s) * 100$. $SF = 100\%$ corresponds to a constant current direction. The small stability factor confirms the great variability of the flow. Values greater than 50% can be observed only at N6 and N7 where the topography of the Norwegian Trench stabilizes the direction of the flow. With a few exceptions in the upper 30 metres of the water column and at N7 at a depth of 256 m, the eddy kinetic energy k_E, which parameterizes the energy of the (low-passed) current fluctuations, exceeds the mean kinetic energy k_M[1]. Vertically, the shear of the mean current direction is relatively small. Near the bottom of the Norwegian Trench, there is a southward and southeastward counter-current at N7 and N8 respectively (Fig. 2).

2.2 *The MOVENS section (September/October 1986)*

The line of MOVENS moorings crosses the northern opening of the Norwegian Trench. Here, the NCC outflow meets the North Atlantic Current which roughly follows the 200 m isobath. Both currents, now known as the Norwegian Current, continue northeastwards along the Norwegian coast (see Fig.1). At the eastern edge of the Norwegian Trench (M10), there is a northward outflow throughout the whole water

[1] $k_E = 0.5\,(\overline{u'u'} + \overline{v'v'})$, $k_M = 0.5\,(\bar{u}^2 + \bar{v}^2)$. u and v are the east-west and north-south components of the velocity vector.

column with an estimated volume transport of $6x10^5$ m^3/s between 3° 30' E and 4° 30' E (see Figs. 2 and 3). At M9, the deepest station in the trench, there is an outflow of about $2x10^5$ m^3/s below a depth of 300 m and an inflow of about $4x10^5$ m^3/s above 150 m depth. At M7 there is a northwestward outflow below 200 m and a westward outflow in the upper 150 m. Regarding the general circulation pattern as outlined in figure 1 and the inflow at M8 and at M9 in the upper 150 metres, we would have expected an inflow of AW at M7 at least in the upper 100 metres. However, there is an outflow from September 7 to September 29. Thereafter the current rotates slowly anticyclonically, reaching its initial (outflow!) direction on October 12. With the exception of the first few days the distinct directional tidal signal is suppressed and the (scalar) velocity is enhanced (see Fig. 4b). This pattern can be observed in all sampling depths at M7. For comparison, Figure 4 shows the unfiltered time series of M8, M7, and M9 in 286 m, 288 m, and 300 m depths, respectively. Evident are the directional stability at M8 at the western slope of the trench (Fig.4c) and the great directional variability at M9, close to the center of the broad opening of the Norwegian Trench (Fig.4a). Here the time series shows a steady succession of eddy structures, rotating both cyclonically and anticyclonically. These current structures represent a signal which is evident in all depth levels. Especially in 240 m depth the low-passed current is extremly variable with a stability factor of only 9% and negligible volume transport (see Table 3).

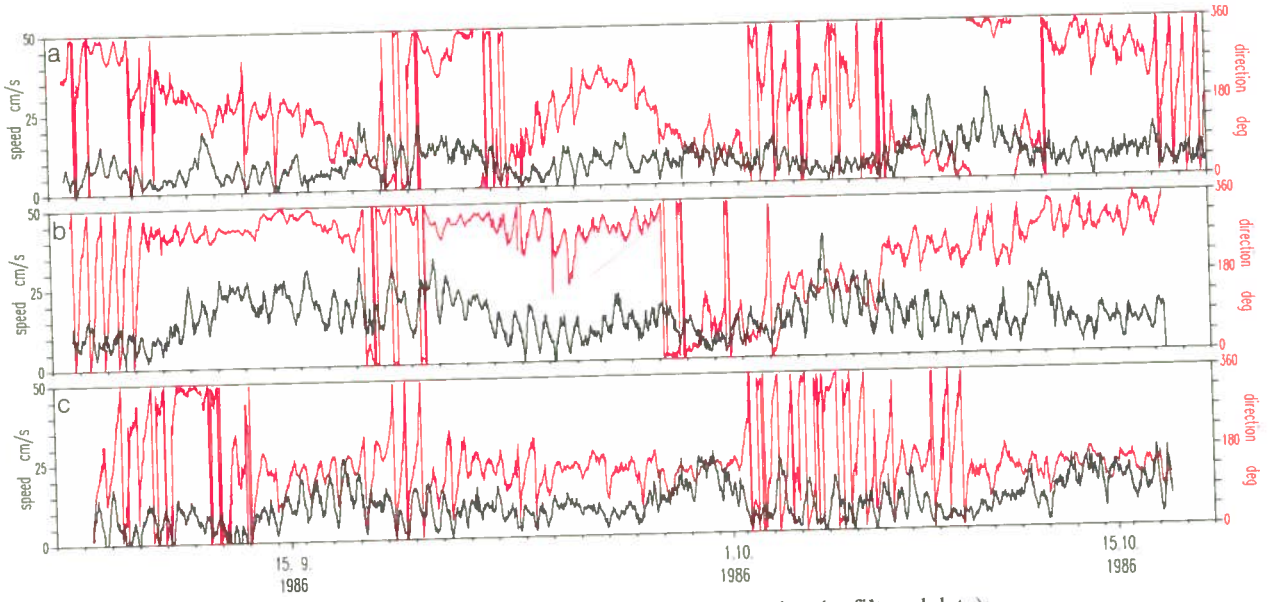

Fig. 4 Time series of current speed and direction (unfiltered data):
a) M9, 300 m sampling depth,
b) M7, 288 m sampling depth,
c) M8, 286 m sampling depth.

The M6 mooring was positioned about 60.5° N at the western edge of the Norwegian Trench. There is an inflow of AW down to a depth of about 250 m, but close to the bottom we observe an outflow like that at M9. In general, the stability factor is less than 32%.

3 Tidal Streams and Tides

3.1 Relating Tidal Streams to Aberdeen as the Port of Reference

The previous part mainly dealt with low-passed current meter data. Residual currents are shown to visualize the general in- and outflow pattern and the respective volume transports are estimated. This part focusses on tidal streams and elevations. Firstly, we give a more qualitative description of the tidal streams and the variation of tidal stream figures along our sections. In a more quantitative approach we determine up to 17 tidal constituents by means of harmonic analysis. Our analysis of observed tidal elevations will be compared to model results.

Methods:

At many locations where stream and tide are both semi-diurnal, there is a definite relation between the times and directions of the tidal stream and the times of high and low water. It is difficult to visualize the tidal stream conditions using the harmonic tidal constituents calculated for the stream components (east-west, north-south). The following procedure is therefore used: the time series of stream components are smoothed by means of spline functions to eliminate current oscillations with periods shorter than 1.5 hours. From 6 hours before until 6 hours after each high water (HW) at Aberdeen, the stream components are determined by means of approximating splines at hourly intervals. This yields 13 pairs of components for each HW. Currents with periods longer than a semi-diurnal cycle are eliminated by subtracting the mean over the 13 values of each current component from the individual values.

The NORA data cover about 60 HWs, i.e. there are 60 pairs of components for each of the 13 hours from 6 hours before until 6 hours after HW Aberdeen. The relationship between each stream component at the measuring station and the coincident tidal range at Aberdeen is estimated by a least squares linear regression. The regression equation is used to calculate mean spring and neap rates of the components from the mean spring and neap tidal ranges at Aberdeen. Taken together, they give the speed and direction of the tidal stream at hourly intervals from 6 hours before until 6 hours after HW Aberdeen for spring and neap conditions. Results of the measurements between 20 and 25 m depth at positions N1 to N4 are given as examples in Table 4.

Table 4

Direction and speed of tidal streams from 6 hours before to 6 hours after high water at Aberdeen betweeen 20 and 25 m depth at positions N1 to N2 during spring and neap time

	SPRING		NEAP		SPRING		NEAP	
time	dir.	speed	dir.	speed	dir.	speed	dir.	speed
h	°	cm/s	°	cm/s	°	cm/s	°	cm/s
	N1 water depth 24 m				**N3 water depth 25 m**			
–6	69	27.2	64	16.6	23	22.0	29	13.8
–5	131	30.3	102	16.1	81	15.9	86	11.4
–4	158	49.2	138	17.9	130	19.9	124	15.5
–3	178	63.2	167	22.8	151	25.3	150	18.7
–2	194	62.6	179	26.8	164	29.2	166	18.2
–1	208	50.7	197	24.4	176	28.2	172	16.9
0	229	32.6	218	16.1	201	24.1	198	15.3
1	294	26.9	269	12.2	260	20.0	249	11.6
2	336	41.7	308	17.0	306	22.1	298	14.4
3	352	57.8	335	23.2	329	28.2	327	16.8
4	3	65.0	348	25.5	330	20.7	334	18.7
5	17	55.5	6	23.1	5	20.6	352	15.0
6	47	35.2	34	17.8	13	23.9	21	15.6
	N2 water depth 22 m				**N4 water depth 22 m**			
–6	29	16.9	45	8.0	17	15.6	33	7.1
–5	101	14.6	118	9.7	69	9.7	97	5.0
–4	136	24.5	148	12.6	143	13.8	146	6.3
–3	147	33.0	148	15.8	157	18.3	179	10.5
–2	161	36.1	157	15.8	159	20.8	182	13.1
–1	175	31.5	165	14.0	171	21.8	185	13.3
0	200	23.1	188	9.6	188	19.0	191	10.0
1	263	17.5	222	5.2	217	16.5	214	6.4
2	309	22.0	311	10.3	288	11.7	335	4.9
3	330	29.9	321	17.2	332	17.1	354	11.7
4	337	35.2	333	18.0	348	22.0	358	14.2
5	347	31.1	343	15.2	354	22.4	8	13.3
6	12	20.1	10	10.8	7	17.7	30	9.5

NORA results:

The tidal stream vectors for spring conditions indicate how the tidal streams change and decrease with increasing distance from the Orkney Islands (Fig. 5). Mean maximum spring speeds near the surface decrease from 65 cm/s at 24 m depth at position N1 to 17 cm/s at 15 m depth at position N7 of the NORA section (Fig. 6). The corresponding mean maximum neap velocities, which are mostly about half as great as the maximum spring ones, decrease from 27 cm/s in the west to about 13 cm/s in the east. The vertical distribution of spring and neap velocities along the NORA section indicates that the strength of the tidal stream is almost vertically homogeneous throughout the whole of the water column. The stream is weakened by bottom friction only near the seabed.

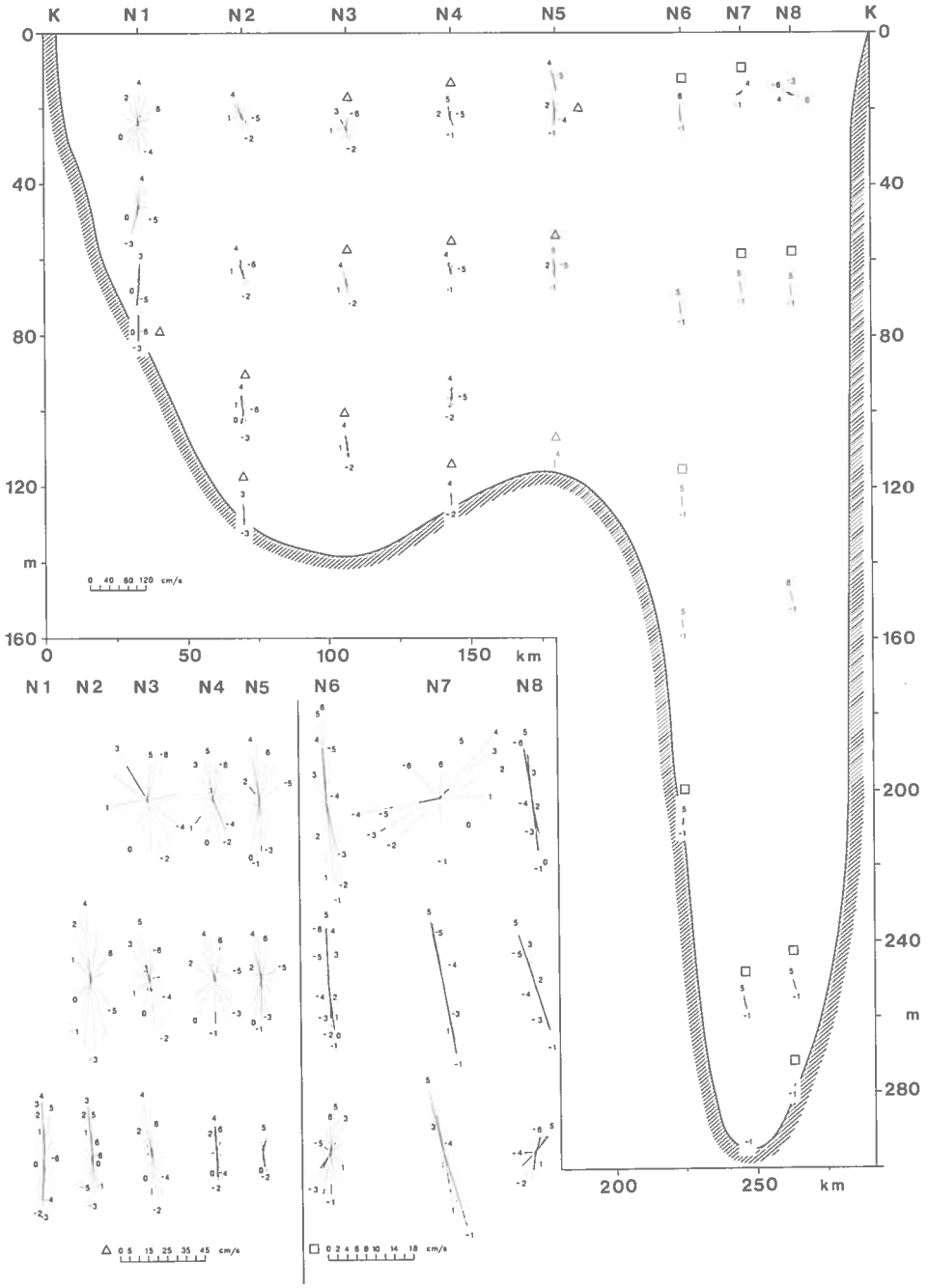

Fig. 5 Spring tidal stream figures in the NORA section, representing speed and direction (north up) from 6 hours before until 6 hours after highwater Aberdeen. To obtain a general view, a uniform scale is kept within the section. Some stream figures, denoted by □ and △, have been enlarged (below left).

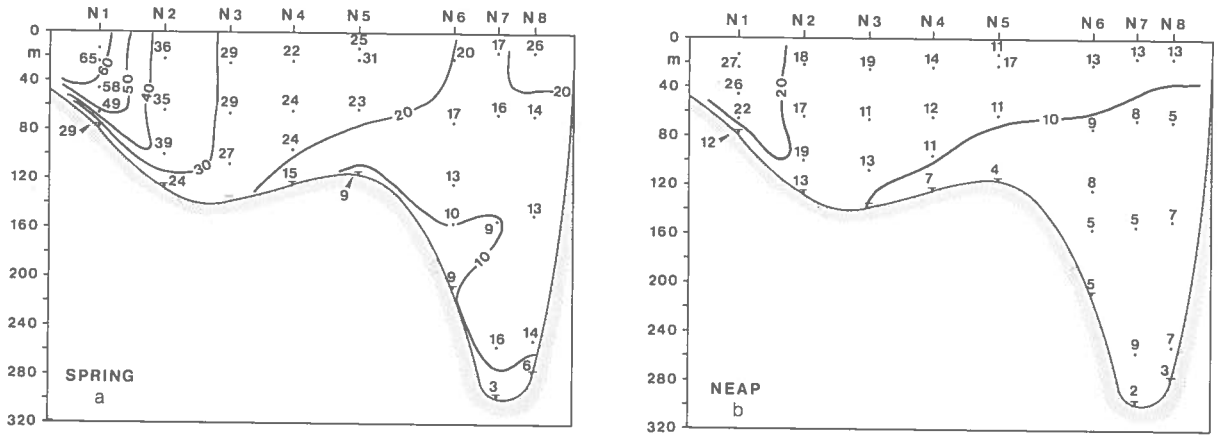

Fig. 6 Mean maximum spring (a) and neap (b) speeds in cm/s in the NORA section.

Tide and tidal streams in the northern North Sea resemble a progressive wave; the strongest northward streams occur around the time of local low water, the strongest southward ones at about local HW. Slack water or time of minimum speed is about 3 hours before and after local HW. At 59° N, eastwards off the Orkneys, HW occurs about 3 hours earlier than in Aberdeen. With regard to the tidal stream figures at Aberdeen, account must be taken of these three hours if the progressive wave character is to be recognized.

The tidal stream at 2° E is approximately half an hour behind the tidal stream near the Orkney Islands at 2° W. Nearing the bottom, the rotating tidal stream becomes more and more alternating. The stream ellipses do not show a distinct vertical phase shift and the phase shift between spring and neap conditions is small (<0.5 hours). This is valid for the NORA section between 2° W and 2° E. In the Norwegian Trench, where the tidal streams are mostly alternating, the situation is not as clear as in areas to its west. In the case of rotational currents, for example near the surface at N7 and N8, the streams rotate both clockwise and anticlockwise and even change their sense of rotation from spring to neap tide. In general, the tidal streams in the Norwegian Trench occur about one hour later than those off the Orkneys.

MOVENS results:

In the MOVENS area the tidal streams have considerable diurnal inequalities, so the tidal currents cannot be related to the semi-diurnal tides at Aberdeen or Bergen. Synthesizing the tidal streams from harmonic constituents yields maximum speeds (speeds connected with the higher HW during spring time) of less than 10 cm/s in the MOVENS area. The maximum tidal stream slightly exceeds 10 cm/s only at a depth of 55 m at position M10, the MOVENS station nearest the Norwegian coast.

3.2 Harmonic Analysis: Tidal Streams

The length of our measurements allows a harmonic analysis which resolves the 17 constituents given in Table 5 for the current measurement at 24 m depth at position N1. For all other time series, only those constituents are listed which have amplitudes greater than 1 cm/s for at least one of both stream components. The method of harmonic tidal analysis assumes that the tide at every location is formed by the same constituents as the equilibrium tide, and that the periods of these terrestrial constituents are those of the equilibrium constituents. Every terrestrial constituent, however, lags behind its corresponding equilibrium constituent. The phases of the equilibrium constituents at 0 hour on 1st January each year have been computed for several years in advance and are published, for example, by DHI [1967]. From the phase of a constituent at 0 hour on 1st January and its known period, its phase can be computed for any time and day. The value of the constituent equals $H\cos(E-G)$, with H the local amplitude of the constituent, E the phase of the equilibrium constituent at the chosen time, and G the local phase lag of the constituent. H and G have been evaluated from the components of all NORA and MOVENS time series according to Pansch [1988].

Table 5

Amplitude and phase of tidal constituents calculated from the east- and north components of the NORA and MOVENS current measurements

N1	Sampling depth = 24 m				Sampling depth = 46 m				Sampling depth = 66 m				Sampling depth = 78 m			
	EC		NC		EC		NC		EC		NC		EC		NC	
80 m	*H*	*G*	*H*	*G*	*H*	*G*	*H*	*G*	*H*	*G*	*H*	*G*	*H*	*G*	*H*	*G*
Q_1	.33	29	.94	114	–	–	–	–	–	–	–	–	–	–	–	–
O_1	.74	208	3.08	176	.65	228	3.12	176	.91	272	3.67	175	.75	294	2.01	174
M_1	.61	322	.05	13	–	–	–	–	–	–	–	–	–	–	–	–
K_1	.71	104	3.29	5	1.13	146	3.33	3	.84	162	3.55	7	.71	172	2.34	12
J_1	.31	95	.80	333	–	–	–	–	–	–	–	–	–	–	–	–
MNS_2	1.53	307	1.08	248	–	–	–	–	–	–	–	–	–	–	–	–
μ_2	1.94	71	1.90	46	2.23	356	.81	37	–	–	–	–	–	–	–	–
N_2	2.66	193	7.19	109	1.30	152	6.27	100	2.01	148	6.90	89	1.52	143	4.71	90
M_2	18.90	225	43.70	136	14.52	199	35.77	130	5.51	173	34.71	122	1.39	154	20.03	118
L_2	1.25	316	1.11	195	1.00	337	.69	202	1.36	150	1.63	90	1.55	134	1.70	80
S_2	7.30	263	17.59	183	5.02	230	14.53	179	1.22	228	12.19	175	.53	314	7.17	177
MSN_2	1.25	196	2.42	124	1.85	120	1.49	95	–	–	–	–	–	–	–	–
$2SM_2$	1.28	283	1.78	229	–	–	–	–	1.28	92	1.16	4	1.19	71	1.17	338
M_4	1.76	99	1.19	317	4.02	105	.39	57	.81	53	.92	354	–	–	–	–
MS_4	1.42	194	.18	16	2.25	132	.64	97	–	–	–	–	–	–	–	–
M_6	1.17	146	.80	87	1.41	40	1.46	21	–	–	–	–	–	–	–	–
$2MS_6$	.25	193	.44	129	1.08	40	1.17	69	–	–	–	–	–	–	–	–
	F = 0.06		*F* = 0.10		*F* = 0.14		*F* = 0.13		*F* = 0.26		*F* = 0.15		*F* = 0.76		*F* = 0.16	

N2	Sampling depth = 22 m				Sampling depth = 63 m				Sampling depth = 100 m				Sampling depth = 127 m			
	EC		NC		EC		NC		EC		NC		EC		NC	
129 m	*H*	*G*	*H*	*G*	*H*	*G*	*H*	*G*	*H*	*G*	*H*	*G*	*H*	*G*	*H*	*G*
O_1	.76	304	2.36	192	.33	302	1.85	170	.25	11	2.15	188	.64	9	1.64	189
K_1	.92	266	1.38	350	.86	224	1.90	4	.56	221	2.58	5	.99	211	1.79	8
MNS_2	1.54	291	1.34	207	1.34	184	.37	60	.37	49	1.06	308	–	–	–	–
μ_2	1.43	244	1.68	166	–	–	–	–	1.59	69	.88	345	–	–	–	–
N_2	2.88	250	3.61	106	2.45	246	3.17	106	1.47	174	4.56	91	.87	223	3.18	101
M_2	13.73	280	24.60	149	10.97	273	23.80	142	7.20	240	27.64	130	1.35	318	18.18	119
L_2	1.30	327	.37	205	1.10	318	.62	215	.83	194	1.28	131	.24	175	1.07	149
S_2	4.17	310	8.47	198	3.91	318	8.85	191	2.46	283	9.95	180	.28	358	6.83	173
MSN_2	1.18	221	.73	160	–	–	–	–	–	–	–	–	–	–	–	–
$2SM_2$	1.03	181	.11	353	1.09	154	.34	30	–	–	–	–	–	–	–	–
M_4	.26	135	1.05	290	–	–	–	–	1.07	91	.40	29	–	–	–	–
	F = 0.09		*F* = 0.11		*F* = 0.08		*F* = 0.11		*F* = 0.08		*F* = 0.13		*F* = 1.00		*F* = 0.14	

Tab. 5 cont.

N3 138 m	Sampling depth = 25 m EC		Sampling depth = 25 m NC		Sampling depth = 66 m EC		Sampling depth = 66 m NC		Sampling depth = 109 m EC		Sampling depth = 109 m NC	
	H	*G*	*H*	*G*	*H*	*G*	*H*	*G*	*H*	*G*	*H*	*G*
O_1	.09	206	1.00	213	.30	303	2.27	195	.41	333	2.22	203
K_1	.55	186	1.44	23	.39	248	1.70	11	.76	239	2.04	16
MNS_2	3.88	281	3.11	219	–	–	–	–	–	–	–	–
μ_2	.84	58	1.69	236	–	–	–	–	–	–	–	–
N_2	2.55	216	3.20	129	1.13	262	3.83	124	1.38	237	4.18	112
M_2	13.52	266	22.26	155	6.54	289	17.01	159	3.95	278	17.18	146
L_2	1.65	290	3.14	200	–	–	–	–	–	–	–	–
S_2	4.28	320	5.89	206	2.25	336	6.71	213	.88	289	5.77	191
MSN_2	1.62	291	1.22	229	–	–	–	–	–	–	–	–
$2SM_2$	.51	286	.93	140	–	–	–	–	–	–	–	–
M_4	1.01	9	1.58	136	–	–	–	–	–	–	–	–
MS_4	.08	344	1.48	184	–	–	–	–	–	–	–	–
M_6	.77	320	2.49	276	–	–	–	–	.50	187	1.50	74
$2MS_6$	.49	80	1.63	315	.43	335	1.03	172	.51	241	1.37	143
	F = 0.04		*F* = 0.09		*F* = 0.08		*F* = 0.17		*F* = 0.24		*F* = 0.19	

N4 125 m	Sampling depth = 22 m EC		Sampling depth = 22 m NC		Sampling depth = 63 m EC		Sampling depth = 63 m NC		Sampling depth = 96 m EC		Sampling depth = 96 m NC		Sampling depth = 123 m EC		Sampling depth = 123 m NC	
	H	*G*	*H*	*G*	*H*	*G*	*H*	*G*	*H*	*G*	*H*	*G*	*H*	*G*	*H*	*G*
O_1	.18	287	1.24	214	.26	137	1.57	189	.24	236	1.53	195	.17	321	1.08	191
K_1	.55	84	1.97	6	.77	286	1.01	1	.72	291	1.29	12	.52	270	1.01	13
μ_2	3.72	273	3.08	206	.79	71	1.24	286	1.54	93	1.01	352	–	–	–	–
N_2	1.47	219	3.02	123	1.22	225	2.83	146	1.46	206	3.51	130	.57	269	1.86	127
M_2	7.05	260	18.52	161	7.43	270	17.02	163	4.57	242	16.20	154	1.28	268	10.56	146
L_2	.76	275	1.22	209	–	–	–	–	–	–	–	–	–	–	–	–
S_2	1.29	314	4.93	209	3.50	313	6.15	208	2.67	287	6.46	206	.87	312	3.98	198
MSN_2	1.55	70	.52	302	–	–	–	–	–	–	–	–	–	–	–	–
M_4	.85	5	1.87	290	–	–	–	–	–	–	–	–	–	–	–	–
MS_4	.57	16	1.07	339	1.15	302	.63	266	–	–	–	–	–	–	–	–
	F = 0.09		*F* = 0.14		*F* = 0.09		*F* = 0.11		*F* = 0.13		*F* = 0.12		*F* = 0.32		*F* = 0.14	

Tab. 5 cont.

N5 116 m	Sampling depth = 13 m				Sampling depth = 21 m				Sampling depth = 62 m				Sampling depth = 114 m			
	EC		NC		EC		NC		EC		NC		EC		NC	
	H	*G*	*H*	*G*	*H*	*G*	*H*	*G*	*H*	*G*	*H*	*G*	*H*	*G*	*H*	*G*
Q_1	–	–	–	–	.83	67	1.52	31	–	–	–	–	–	–	–	–
O_1	.71	87	1.56	222	.47	88	2.05	218	.10	190	1.75	182	–	–	–	–
K_1	.85	100	2.00	350	1.02	72	1.39	338	–	–	–	–	–	–	–	–
MNS_2	.86	249	2.29	131	2.56	200	2.83	126	–	–	–	–	–	–	–	–
μ_2	.80	19	1.11	157	2.78	266	1.22	228	–	–	–	–	–	–	–	–
N_2	1.94	305	4.00	117	2.02	193	2.91	123	1.37	197	2.98	138	.50	287	1.47	137
M_2	4.56	324	16.68	164	5.52	242	23.44	165	3.74	256	16.78	164	.14	333	6.15	154
L_2	1.20	214	1.91	21	1.34	112	.67	309	–	–	–	–	–	–	–	–
S_2	1.43	343	5.84	200	1.95	258	8.47	205	1.86	319	6.25	221	.31	310	2.29	207
MSN_2	–	–	–	–	2.57	52	2.68	23	–	–	–	–	–	–	–	–
$2SM_2$	.95	36	2.34	218	1.76	324	2.22	185	–	–	–	–	–	–	–	–
M_4	–	–	–	–	1.04	113	.93	255	–	–	–	–	–	–	–	–
MS_4	.72	114	1.25	347	1.07	113	1.17	350	–	–	–	–	–	–	–	–
M_6	.61	246	1.00	354	.95	35	1.36	335	–	–	–	–	–	–	–	–
$2MS_6$	–	–	–	–	.90	17	1.29	11	–	–	–	–	–	–	–	–
	$F = 0.26$		$F = 0.16$		$F = 0.20$		$F = 0.11$									

N6 210 m	Sampling depth = 21 m				Sampling depth = 73 m				Sampling depth = 124 m				Sampling depth = 156 m				Sampling depth = 208 m			
	EC		NC		EC		NC		EC		NC		EC		NC		EC		NC	
	H	*G*	*H*	*G*	*H*	*G*	*H*	*G*	*H*	*G*	*H*	*G*	*H*	*G*	*H*	*G*	*H*	*G*	*H*	*G*
O_1	.64	118	1.35	270	1.67	163	1.18	287	–	–	–	–	1.31	137	.45	214	–	–	–	–
M_1	.52	39	1.24	163	1.55	102	.25	151	–	–	–	–	–	–	–	–	–	–	–	–
K_1	.36	5	1.11	18	2.11	300	.82	14	1.22	283	.57	44	1.16	304	.46	45	–	–	–	–
MNS_2	3.38	275	3.03	196	1.32	75	.97	17	–	–	–	–	–	–	–	–	–	–	–	–
μ_2	2.04	183	2.06	113	1.46	257	1.15	287	.47	334	1.07	331	1.29	80	.13	350	–	–	–	–
N_2	1.24	126	1.19	94	2.14	292	3.62	180	.38	241	2.15	151	.36	246	1.36	131	.65	102	1.28	119
M_2	4.06	329	15.18	193	2.17	89	12.31	179	1.69	59	9.09	181	1.73	42	6.25	179	1.92	93	6.35	160
L_2	–	–	–	–	.31	274	2.15	261	–	–	–	–	–	–	–	–	–	–	–	–
S_2	.96	145	3.97	220	1.89	47	3.44	226	.33	300	3.22	226	.54	295	2.64	236	.27	148	2.38	216
MSN_2	1.45	320	.28	99	1.56	157	.31	144	–	–	–	–	–	–	–	–	–	–	–	–
$2SM_2$	3.03	285	4.23	202	.86	346	1.04	79	–	–	–	–	–	–	–	–	–	–	–	–
M_4	.29	110	1.31	82	.58	144	1.03	319	–	–	–	–	–	–	–	–	–	–	–	–
MS_4	1.40	351	.28	284	.13	179	1.53	68	–	–	–	–	–	–	–	–	–	–	–	–
	F = 0.20		F = 0.13		F = 0.93		F = 0.13						$F = 1.09$		$F = 0.10$					

Tab. 5 cont.

N7 295 m	Sampling depth = 15 m EC		Sampling depth = 15 m NC		Sampling depth = 67 m EC		Sampling depth = 67 m NC		Sampling depth = 256 m EC		Sampling depth = 256 m NC		Sampling depth = 293 m EC		Sampling depth = 293 m NC	
	H	*G*	*H*	*G*	*H*	*G*	*H*	*G*	*H*	*G*	*H*	*G*	*H*	*G*	*H*	*G*
Q_1	1.11	67	.80	77	–	–	–	–	–	–	–	–	–	–	–	–
O_1	.71	74	2.24	238	–	–	–	–	.64	95	1.26	252	–	–	–	–
M_1	1.61	3	1.58	186	–	–	–	–	–	–	–	–	–	–	–	–
K_1	.43	333	1.65	35	.70	258	1.01	59	.42	297	1.20	50	–	–	–	–
MNS_2	1.95	309	1.84	206	–	–	–	–	–	–	–	–	–	–	–	–
μ_2	8.60	27	5.98	283	–	–	–	–	–	–	–	–	–	–	–	–
N_2	1.98	147	2.87	107	.29	350	2.15	155	.56	270	2.39	147	–	–	–	–
M_2	4.29	108	9.63	158	1.72	354	10.42	182	2.99	355	11.58	188	.45	78	1.43	13
L_2	1.62	312	2.38	229	–	–	–	–	–	–	–	–	–	–	–	–
S_2	2.54	157	5.27	196	.65	27	3.37	232	.83	89	2.92	234	–	–	–	–
MSN_2	2.30	196	3.56	106	–	–	–	–	–	–	–	–	–	–	–	–
$2SM_2$	3.42	169	1.37	113	–	–	–	–	–	–	–	–	–	–	–	–
	$F = 0.17$		$F = 0.26$						$F = 0.28$		$F = 0.17$					

N8 280 m	Sampling depth = 16 m EC		Sampling depth = 16 m NC		Sampling depth = 68 m EC		Sampling depth = 68 m NC		Sampling depth = 149 m EC		Sampling depth = 149 m NC		Sampling depth = 251 m EC		Sampling depth = 251 m NC		Sampling depth = 278 m EC		Sampling depth = 278 m NC	
	H	*G*	*H*	*G*	*H*	*G*	*H*	*G*	*H*	*G*	*H*	*G*	*H*	*G*	*H*	*G*	*H*	*G*	*H*	*G*
Q_1	.66	171	1.05	165	–	–	–	–	–	–	–	–	–	–	–	–	–	–	–	–
O_1	.73	84	1.86	251	–	–	–	–	.57	75	1.20	261	–	–	–	–	–	–	–	–
M_1	.51	217	2.39	188	–	–	–	–	–	–	–	–	–	–	–	–	–	–	–	–
K_1	.33	335	1.42	108	.46	349	1.21	78	–	–	–	–	.84	265	1.04	67	–	–	–	–
MNS_2	4.30	283	4.49	185	–	–	–	–	–	–	–	–	–	–	–	–	–	–	–	–
μ_2	6.75	342	7.37	265	.91	211	1.15	99	–	–	–	–	–	–	–	–	–	–	–	–
N_2	2.65	263	4.26	169	1.04	119	1.79	104	.76	327	1.62	150	.80	359	1.21	142	–	–	–	–
M_2	13.39	17	11.05	237	2.28	32	8.71	185	2.40	360	9.23	185	2.56	1	9.04	175	1.32	138	3.59	168
L_2	3.66	39	3.76	302	–	–	–	–	–	–	–	–	–	–	–	–	–	–	–	–
S_2	6.05	90	3.73	341	.37	29	3.35	237	.83	67	3.14	238	1.00	19	3.36	220	.70	202	1.30	212
MSN_2	1.14	99	.81	5	.67	245	1.17	163	–	–	–	–	–	–	–	–	–	–	–	–
$2SM_2$	2.94	330	2.03	262	–	–	–	–	–	–	–	–	–	–	–	–	–	–	–	–
M_4	2.02	66	1.27	353	–	–	–	–	–	–	–	–	–	–	–	–	–	–	–	–
	$F = 0.05$		$F = 0.22$																	

Tab. 5 cont.

M7 375 m	Sampling depth = 70 m EC		Sampling depth = 70 m NC		Sampling depth = 120 m EC		Sampling depth = 120 m NC		Sampling depth = 225 m EC		Sampling depth = 225 m NC		Sampling depth = 288 m EC		Sampling depth = 288 m NC		Sampling depth = 365 m EC		Sampling depth = 365 m NC	
	H	*G*	*H*	*G*	*H*	*G*	*H*	*G*	*H*	*G*	*H*	*G*	*H*	*G*	*H*	*G*	*H*	*G*	*H*	*G*
O_1	.93	340	1.75	252	1.05	24	1.77	243	1.17	301	2.09	235	1.45	279	2.06	232	1.18	261	1.88	218
M_1	–	–	–	–	–	–	–	–	–	–	–	–	–	–	–	–	1.12	314	.50	289
K_1	–	–	–	–	1.01	195	.84	49	1.04	108	1.44	29	.44	108	1.35	47	.56	62	1.55	29
μ_2	–	–	–	–	–	–	–	–	–	–	–	–	.91	147	1.05	66	1.18	20	1.08	293
MNS_2	1.14	271	.74	188	–	–	–	–	–	–	–	–	–	–	–	–	–	–	–	–
N_2	1.09	340	.42	274	–	–	–	–	–	–	–	–	1.38	246	1.25	160	1.42	148	.81	64
M_2	1.87	281	1.52	205	1.43	304	1.85	207	3.13	286	2.64	195	3.35	266	2.86	176	1.91	207	1.27	121
S_2	1.87	329	.92	210	1.10	347	.93	191	1.64	312	.92	209	1.48	307	.96	205	–	–	–	–
					$F = 0.81$		$F = 0.94$		$F = 0.46$		$F = 0.99$		$F = 0.39$		$F = 0.89$					

M8 355 m	Sampling depth = 90 m EC		Sampling depth = 90 m NC		Sampling depth = 163 m EC		Sampling depth = 163 m NC		Sampling depth = 226 m EC		Sampling depth = 226 m NC		Sampling depth = 286 m EC		Sampling depth = 286 m NC		Sampling depth = 348 m EC		Sampling depth = 348 m NC	
	H	*G*	*H*	*G*	*H*	*G*	*H*	*G*	*H*	*G*	*H*	*G*	*H*	*G*	*H*	*G*	*H*	*G*	*H*	*G*
O_1	1.59	257	2.41	193	2.19	204	1.71	265	1.26	317	1.92	205	1.61	256	2.36	206	1.19	257	2.79	200
M_1	–	–	–	–	–	–	–	–	1.15	117	.37	335	–	–	–	–	.96	49	1.01	237
K_1	1.04	45	1.45	349	1.60	3	.82	51	.71	191	1.38	9	.79	51	1.78	6	.62	32	1.88	359
μ_2	1.31	149	1.18	50	1.02	211	1.08	303	–	–	–	–	–	–	–	–	–	–	–	–
N_2	1.29	232	1.45	140	–	–	–	–	–	–	–	–	.96	238	1.06	140	–	–	–	–
M_2	3.78	299	2.67	207	2.36	184	2.23	281	1.53	291	1.64	171	3.58	260	2.70	156	2.43	210	1.73	84
S_2	1.78	304	.77	187	1.19	210	2.04	314	1.17	333	1.16	211	2.02	285	1.62	185	1.32	239	.85	119
	$F = 0.47$		$F = 1.12$		$F = 1.07$		$F = 0.59$		$F = 0.73$		$F = 1.18$		$F = 0.43$		$F = 0.96$		$F = 0.48$		$F = 1.81$	

M9 413 m	Sampling depth = 60 m EC		Sampling depth = 60 m NC		Sampling depth = 130 m EC		Sampling depth = 130 m NC		Sampling depth = 240 m EC		Sampling depth = 240 m NC		Sampling depth = 300 m EC		Sampling depth = 300 m NC		Sampling depth = 403 m EC		Sampling depth = 403 m NC	
	H	*G*	*H*	*G*	*H*	*G*	*H*	*G*	*H*	*G*	*H*	*G*	*H*	*G*	*H*	*G*	*H*	*G*	*H*	*G*
O_1	.80	285	1.36	275	.87	275	1.45	285	.73	281	1.35	283	.71	272	1.72	276	.50	262	1.94	279
M_1	–	–	–	–	–	–	–	–	–	–	–	–	–	–	–	–	.66	61	1.07	19
K_1	.16	175	1.08	71	–	–	–	–	–	–	–	–	.45	48	1.09	47	.38	35	1.25	55
MNS_2	1.61	343	1.71	249	–	–	–	–	–	–	–	–	–	–	–	–	–	–	–	–
μ_2	1.38	156	1.45	72	–	–	–	–	–	–	–	–	–	–	–	–	–	–	–	–
N_2	.83	310	1.11	195	–	–	–	–	–	–	–	–	–	–	–	–	–	–	–	–
M_2	2.43	245	2.85	189	1.28	294	2.03	221	.75	326	1.67	232	1.23	293	2.69	224	1.41	232	1.95	210
S_2	1.02	323	1.15	251	–	–	–	–	–	–	–	–	–	–	–	–	–	–	–	–
	$F = 0.28$		$F = 0.61$																	

Tab. 5 cont.

M10 210 m	Sampling depth = 55 m EC		Sampling depth = 55 m NC		Sampling depth = 75 m EC		Sampling depth = 75 m NC		Sampling depth = 205 m EC		Sampling depth = 205 m NC	
	H	*G*	*H*	*G*	*H*	*G*	*H*	*G*	*H*	*G*	*H*	*G*
Q_1	–	–	–	–	–	–	–	–	.54	105	1.02	198
O_1	1.74	275	2.93	249	1.79	288	2.47	252	.98	256	3.52	249
M_1	.66	313	1.43	343	1.19	6	2.40	314	.57	67	1.40	314
K_1	1.39	72	2.26	41	1.51	98	1.78	53	.54	73	1.94	42
MNS_2	1.20	34	.80	270	–	–	–	–	–	–	–	–
μ_2	1.96	255	1.46	160	.37	271	1.00	171	–	–	–	–
N_2	–	–	–	–	1.00	248	.95	180	.92	212	1.23	156
M_2	3.12	319	6.66	238	1.17	251	3.03	235	2.83	153	2.14	186
S_2	1.24	218	.79	250	–	–	–	–	.93	220	1.09	211
MSN_2	1.51	336	1.44	251	–	–	–	–	–	–	–	–
$2SM_2$	1.02	302	.72	199	–	–	–	–	–	–	–	–
	F = 0.72		*F* =0.70						*F* = 0.40		*F* = 1.69	

Results are listed only, if the amplitude of one of the two components is greater than 1 cm/s
EC = east component
NC = north component
H = amplitude (cm/s)
G = phase (degree)
F = form ratio $(K_1 + O_1) / (M_2 + S_2)$

The reliability of tidal constituents determined from a single month of data is problematic. The harmonic constituents derived from each time series were therefore synthesized to allow a comparison with the results of the reference to HW Aberdeen. If the time series contain a recognizable tidal signal, both methods yield reliable results. If non-tidal variability dominates, neither method is successful. However, it is simpler to describe local tidal streams by using the relation between the tidal stream and HW at a reference station than by using harmonic analysis and synthesis.

Generally, phase errors increase with decreasing amplitudes of the constituents. The amplitude errors which are less than 1 cm/s are often of the same order of magnitude as the amplitude itself. The amplitude and phase of the M_2 stream constituent presented in this paper can be compared with data published by Davies and Furnes [1980]. Despite large vertical and horizontal variations of amplitudes and phases, there is good agreement: not only with respect to the amplitudes of the components, but also with regard to the phases of the dominant north component. Figure 7 shows the phases of the M_2 and S_2 north components. In our view the number and distribution of data points are insufficient for a more detailed presentation of isolines. As regards the NORA section, the M_2 and S_2 constituents of the north component suggest a phase lag from west to east of about one hour, confirming the delay of the overall tidal stream which is evident in the stream ellipses.

The M_2 and S_2 amplitudes of both stream components in the NORA and MOVENS section are shown in Figure 8. The amplitudes of the north components are at least twice as large as those of the east components in the NORA section except near the surface at position N8. In the MOVENS area, however, the amplitudes of both components are relatively small and are approximately of the same order.

The ratio between the amplitudes of the diurnal constituents K_1 and O_1 and those of the semi-diurnal constituents M_2 and S_2 gives the form ratio *F* which determines the type of the tide:

$$F = (K_1 + O_1)/(M_2 + S_2).$$

If *F* is smaller than 0.25, as is the case for the components of the major stream axis along the NORA section, the tide is semi-diurnal. Values between 0.25 and 1.50 indicate a mixed but mainly semi-diurnal tide with large inequalities in range and time between the high and low waters each day. In the MOVENS section, *F* is larger than 0.3, indicating mixed tidal stream conditions (see Table 5).

Fig. 7 Phase angles of the north component in degree of the M_2 and S_2 constituent:

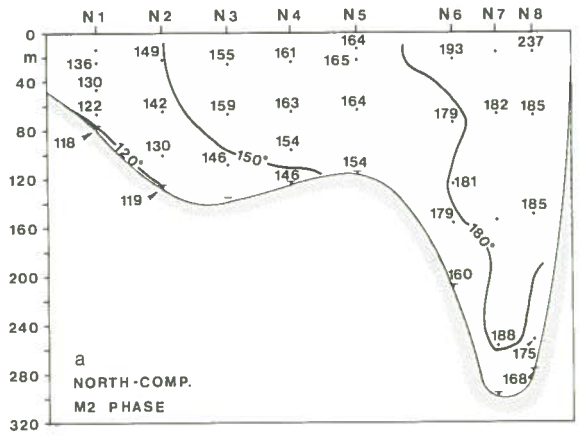

a) M_2 constituent, NORA,

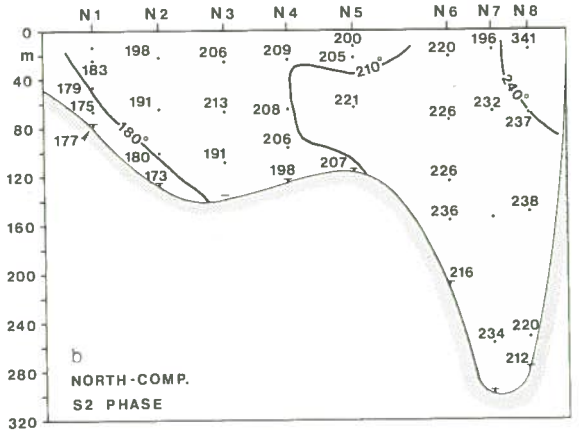

b) S_2 constituent, NORA,

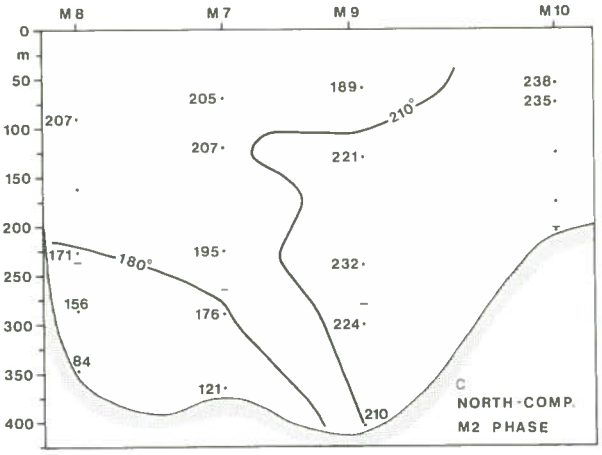

c) M_2 constituent, MOVENS,

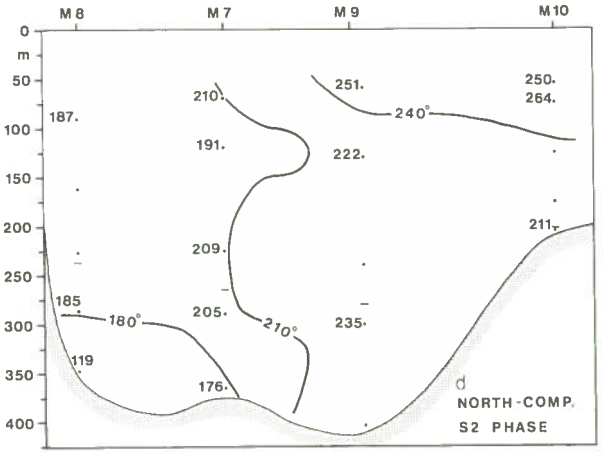

d) S_2 constituent, MOVENS.

Fig. 8 Amplitudes in cm/s of the M_2 and S_2 constituents:

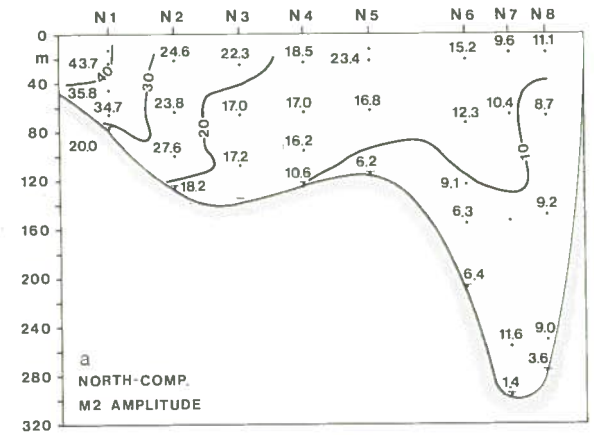

a) M_2 north component, NORA,

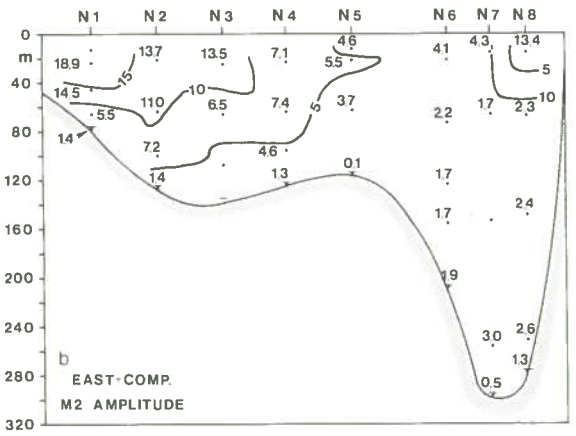

b) M_2 east component, NORA,

Fig. 8 cont.

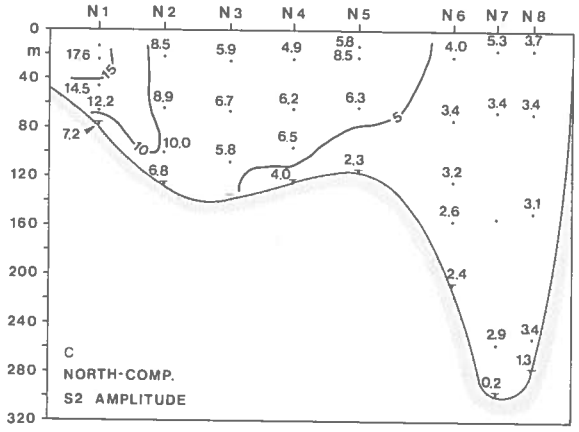

c) S_2 north component, NORA,

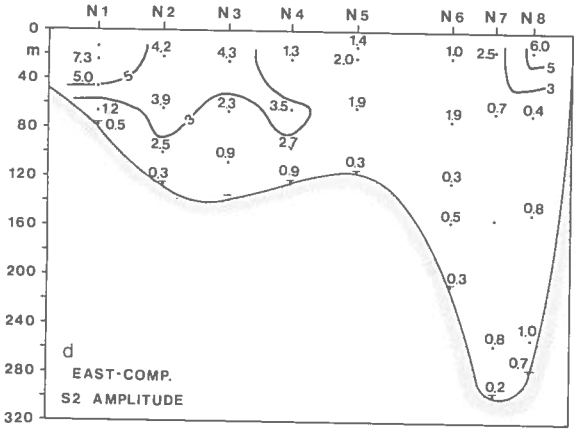

d) S_2 east component, NORA,

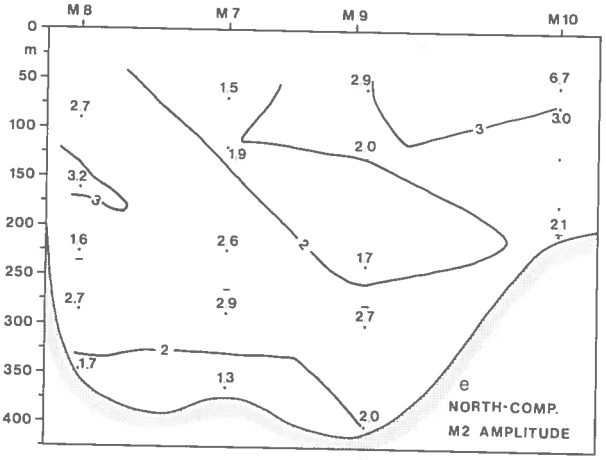

e) M_2 north component, MOVENS,

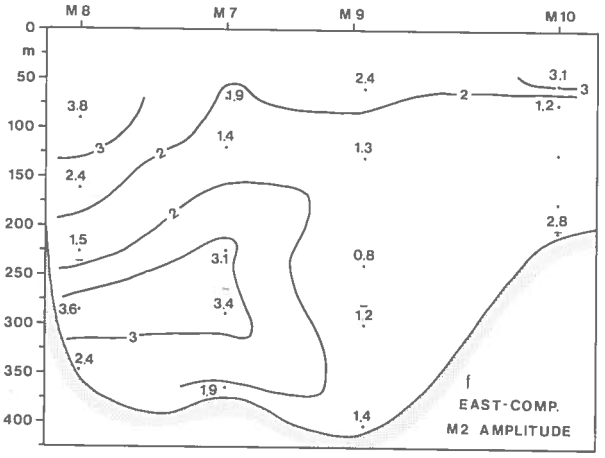

f) M_2 east component, MOVENS,

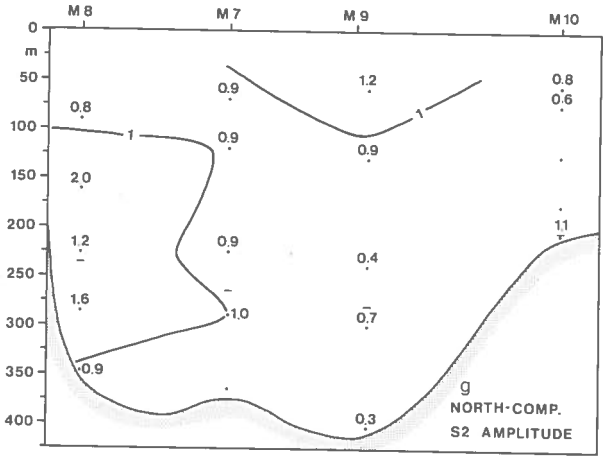

g) S_2 north component, MOVENS,

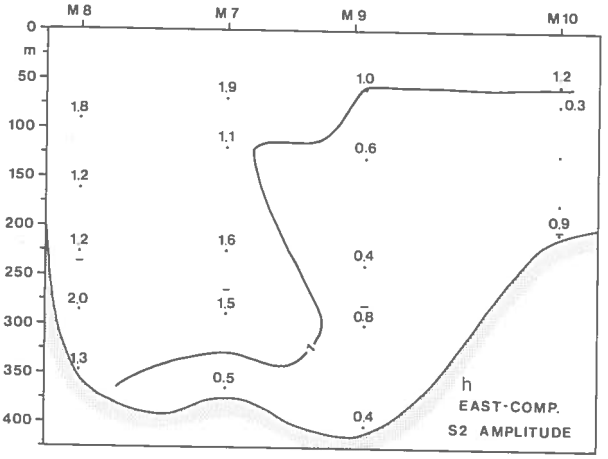

h) S_2 east component, MOVENS.

3.3 *Harmonic Analysis: Elevations*

The results of the harmonic analysis of the water level records are listed in Table 6. Figure 9 shows how the semi-diurnal M_2 and S_2 amplitudes *H* and phases *G* vary from west to east along the NORA section. Data from the "Class A Network Dataring Gauge" at the port of Wick (58° 26.5' N, 3° 05.1' E) are included in Table 6 and Fig. 9 for comparison purposes (S h a w [1992a,b]). Harmonic synthesis calculations by means of the constituents of Table 6 indicate that the tide, as well as the tidal stream, is delayed by about 0.5 hours between 2° W and 2° E. The synthesis shows a mean time lag of about 1.5 hours between the MOVENS and the NORA data. Amplitudes and phases of the Q_1, O_1, K_1, N_2, M_2 and S_2 tidal constituents can be compared with the model results given by S c h w i d e r s k i [1979–1981] (see Table 7). Generally, the NORA amplitudes agree well with Schwiderski's results. Most phase angles agree within a few degrees, but there are some positions with considerable differences, e. g. S_2 at N1. With the exception of the N_2 constituent at M9, the MOVENS amplitudes are definitely larger than the model results. Some of the MOVENS phase angles agree well, other differ up to 126°. The possible reasons for the differing phase angles are the limited length of our time series (about 1 month) and the method used by Schwiderski to model ocean tides.

The M_2 phase along the NORA section agrees better with D a v i s 's results [1981]. As in many papers by other authors, however, Davis investigated only the M_2 tide. Other harmonic constituents cannot therefore be compared.

Table 6

Amplitudes *H* and phase angles *G* of 17 tidal constituents calculated from tide gauge time series of the NORA- and MOVENS section

Constituent	WICK*)		N1		N2		N3		N4		N5		M8		M9	
	H	*G*	*H*	*G*	*H*	*G*	*H*	*G*	*H*	*G*	*H*	*G*	*H*	*G*	*H*	*G*
	cm	°	cm	°	cm	°	cm	°	cm	°	cm	°	cm	°	cm	°
Q_1	3.2	343	2.5	338	2.2	340	1.4	342	1.5	4	1.7	0	3.5	287	5.1	214
O_1	11.7	25	10.0	26	7.9	33	6.0	40	5.5	41	4.6	40	11.1	14	8.9	90
M_1	–	–	1.0	293	1.1	298	0.5	278	1.0	310	1.2	315	3.9	255	15.6	168
K_1	10.8	175	10.6	189	8.8	191	7.0	194	5.7	200	4.6	203	7.6	149	13.1	233
J_1	0.8	240	0.9	210	1.1	196	0.5	192	0.6	232	0.7	214	1.4	194	2.0	153
MNS_2	–	–	0.2	39	1.2	30	0.8	1	0.5	331	0.2	355	4.5	246	8.5	0
μ_2	–	–	1.0	331	0.6	96	1.1	334	1.4	325	1.1	309	3.9	45	5.5	88
N_2	20.3	303	14.1	286	11.3	299	9.7	302	8.1	302	7.0	301	14.5	258	4.2	171
M_2	101.7	322	79.4	314	64.2	318	51.3	328	42.4	329	34.9	326	57.9	295	50.9	295
L_2	–	–	3.4	346	2.9	356	1.9	348	1.6	343	1.7	329	6.0	273	8.0	94
S_2	35.0	0	28.0	7	23.0	11	19.7	20	16.9	19	14.2	17	31.9	316	32.6	320
MSN_2	–	–	1.6	259	1.9	281	0.9	297	0.6	286	1.1	277	5.0	80	7.2	62
$2SM_2$	–	–	2.2	182	1.2	168	1.1	190	0.6	151	0.3	193	2.7	282	7.5	114
M_4	3.6	317	2.8	267	4.3	281	1.6	286	1.4	265	1.3	265	1.3	295	1.7	69
MS_4	2.0	51	0.8	2	2.0	348	1.2	21	1.0	8	0.7	25	1.9	280	1.7	85
M_6	0.6	227	1.2	179	1.0	197	0.7	249	0.5	308	0.7	22	0.3	202	0.7	93
$2MS_6$	–	–	1.0	237	1.1	272	0.8	302	0.6	326	0.3	80	0.4	277	1.3	355
F	0.17		0.19		0.19		0.18		0.19		0.19		0.21		0.26	

$F = (K_1 + O_1) / (M_2 + S_2)$

*) data from Shaw [1992]

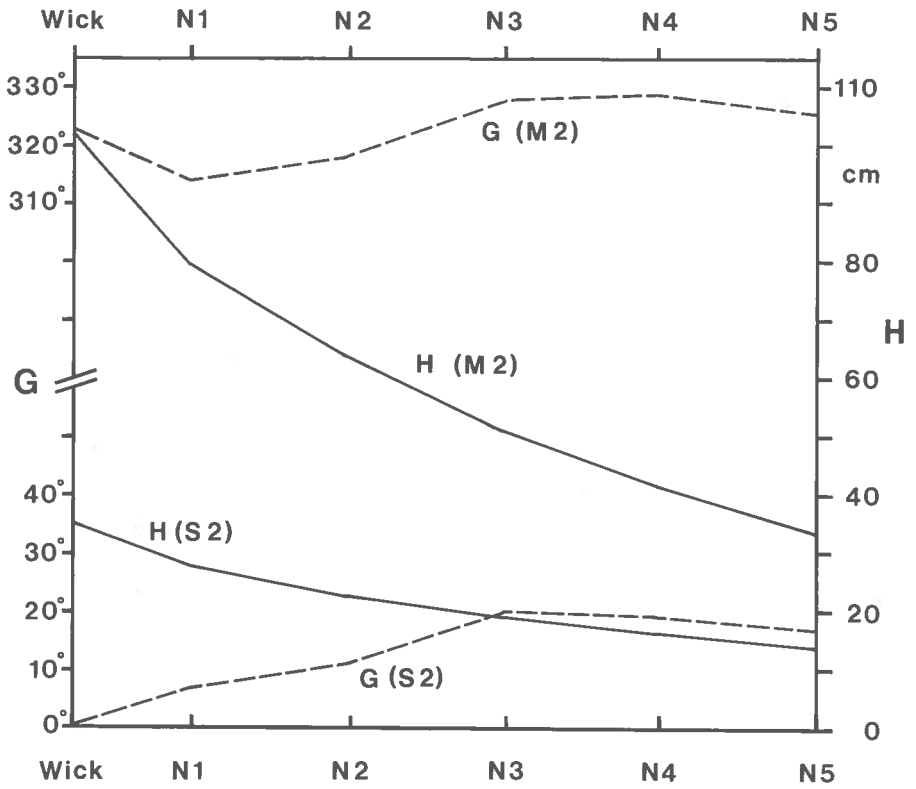

Fig. 9: Phase angles G in degree and amplitudes H in cm of the M_2 and S_2 constituents for tidal elevations in the NORA section.

Table 7

Amplitudes H and phase angles G of 6 tidal constituents calculated from tide gauge time series of the NORA- and MOVENS section and model results from Schwiderski [1979–1981] at the respective positions

Constituent		N1		N2		N3		N4		N5		M8		M9	
		H	*G*	*H*	*G*	*H*	*G*	*H*	*G*	*H*	*G*	*H*	*G*	*H*	*G*
		cm	°	cm	°	cm	°	cm	°	cm	°	cm	°	cm	°
Q_1	NORA/MOVENS	2.5	338	2.2	340	1.4	342	1.5	4	1.7	0	3.5	287	5.1	214
	Schwiderski	3.1	334	2.7	327	2.3	319	2.0	311	1.8	293	2.1	344	1.9	340
O_1	NORA/MOVENS	10.0	26	7.9	33	6.0	40	5.5	41	4.6	40	11.1	14	8.9	90
	Schwiderski	9.0	27	8.0	37	6.5	44	5.5	46	4.5	47	6.0	34	5.5	33
K_1	NORA/MOVENS	10.6	189	8.8	191	7.0	194	5.7	200	4.6	203	7.6	149	13.1	233
	Schwiderski	9.0	171	7.5	177	6.0	185	4.5	192	3.5	191	6.0	167	5.0	169
N_2	NORA/MOVENS	14.1	286	11.3	299	9.7	302	8.1	302	7.0	301	14.5	258	4.2	171
	Schwiderski	15.0	291	12.5	304	10.5	308	8.5	310	6.5	306	9.5	265	9.5	266
M_2	NORA/MOVENS	79.4	314	64.2	318	51.3	328	42.4	329	34.9	326	57.9	295	50.9	295
	Schwiderski	73.5	291	59.5	309	49.0	324	41.0	330	33.0	328	42.5	289	43.5	291
S_2	NORA/MOVENS	28.0	7	23.0	11	19.7	20	16.9	19	14.2	17	31.9	316	32.6	320
	Schwiderski	23.5	326	21.0	351	17.0	3	15.5	8	13.5	4	17.0	319	17.5	321

4 Conclusions

The estimated volume transports agree well with those calculated by the authors cited above. According to Turrell [1992b] the FIC west of Orkney is predominantly wind-driven in summer and winter. However, the inflow of AW east of Shetland has an additional significant non-wind-driven component during the summer months. Variations in wind stress magnitude and direction cause interannual variability of these inflows. For the FIC within the North Sea, Turrell [1992b] estimated a maximum southerly transport of 2.5×10^5 m^3/s in late August, while the NORA data yield 2.6×10^5 m^3/s between mid July and late August.

The unexpected northwestward "residual flow" at the MOVENS mooring M7 and especially the great directional variability at M9 show that short records can be biased by mesoscale instabilities between the AW inflow at the western and the NCC at the eastern edge of the Norwegian Trench. According to Ikeda et al. [1989], these instabilities have a typical wavelength of 50–100 km and northward propagation speeds of 10–20 cm/s, i.e. they would pass a mooring in between 3 to 12 days. This agrees fairly with the observed period of current rotations at M9 which amounts to about 10 days (see Fig. 4a).

The tidal streams at the MOVENS moorings are negligible although the tidal elevations are relatively strong. Further south, at the NORA section, distinct tidal streams and elevations are both observed with increasing magnitude from east to west. The amplitudes of some tidal constituents reach considerable magnitudes. For the main diurnal and semi-diurnal constituents (N_2, S_2, O_1, and K_1, see Table 6), we calculate a relative amplitude H_r, i. e. the ratio between the amplitude of the tidal constituent and the respective M_2-amplidtude, expressed in percent (see Table 8). In the NORA section (N1–N5) no significant change is observed in the relative amplitudes; only the relative S_2 amplitude increases from west to east. At the M8 and M9 moorings the S_2 amplitudes amount to 55 and 64% respectively of the M_2 amplitude. The other constituents at the MOVENS positions are also greater than the corresponding NORA values except for the N2 constituent at M9.

Table 8

Amplitudes H and relative amplitudes H_r of the main diurnal and semi-diurnal tidal constituents of the NORA- and MOVENS section, calculated from tide gauge time series

Constituent	N1		N2		N3		N4		N5		M8		M9	
	H	H_r	H	H_r	H	H_r	H	H_r	H	H_r	H	H_r	H	H_r
	cm	%	cm	%	cm	%	cm	%	cm	%	cm	%	cm	%
M_2	79.4	100	64.2	100	51.3	100	42.4	100	34.9	100	57.9	100	50.9	100
O_1	10.0	13	7.9	12	6.0	12	5.5	13	4.6	13	11.1	19	8.9	17
K_1	10.6	13	8.8	14	7.0	14	5.7	13	4.6	13	7.6	13	13.1	26
N_2	14.1	18	11.3	18	9.7	19	8.1	19	7.0	20	14.5	25	4.2	8
S_2	28.0	35	23.0	36	19.7	38	16.9	40	14.2	41	31.9	55	32.6	64

$H_r = (H(x)/H(M_2)) \times 100$

Our results will next be incorporated as northern boundary values in a numerical circulation model of the North Sea/Baltic Sea. The model results can then be compared with the model's present performance and compared with field observations in the model area.

Acknowledgements

The authors would like to thank the officers and crews of RV *Gauss* and RV *Valdivia* for their help at sea; thanks are also due to Holger May for his excellent drawings.

References

Davies, A.M., 1981: Three Dimensional Hydrodynamic Numerical Models. The Norwegian Coastal Current, **2**, 370–426.

Davies, A.M. and G.K. Furnes, 1980: Observed and Computed Tidal Currents in the North Sea. J. Phys. Oceanogr., **10**, 237–257.

Delhez, E. and G. Martin, 1992: Preliminary results of 3-D baroclinic models of the mesoscale and macroscale circulations on the North-West European Shelf. J. Mar. Systems, **3**, 423–440.

DHI, 1967: Tafeln der Astronomischen Argumente V_o+v und der Korrektionen j, v. Deutsches Hydrographisches Institut, Nr. 2276, 128pp.

Furnes, G.K., B. Hackett and R. Sætre, 1986: Retroflection of Atlanic water in the Norwegian Trench. Deep-Sea Res., **33**, 247–265.

Johannessen, J.A., et al., 1989: Three-dimensional structure of mesoscale eddies in the Norwegian Coastal Current. J. Physical Oceanogr., **19**, 3–19.

Ikeda, M., et al., 1989: A process study of mesoscale meanders and eddies in the Norwegian Coastal Current. J. Physical Oceanogr., **19**, 20–35.

Otto, L., et al., 1990: Review of the physical oceanography of the North Sea. Netherl. J. of Sea Res., **26**, 161–238.

Pansch, E., 1988: Harmonische Analyse von Gezeiten- und Gezeitenstrombeobachtungen im Deutschen Hydrographischen Institut, Hamburg. Interner Technischer Bericht Nr.1/88/M13, 32pp.

Shaw, S.M., 1992a: Class A Network Dataring Gauges, 1990 data processing and analysis. Proudman Oceanographic Laboratory, Report No. 23, 116pp.

Shaw, S.M., 1992b: Class A Network Dataring Gauges, 1991 data processing and analysis. Proudman Oceanographic Laboratory, Report No. 26, 135pp.

Schwiderski, E.W., 1979–1981: Global Ocean Tides, Part 2, 3, 4, 5, 6 and 9. Naval Surface Weapons Center, Dahlgren, Virginia.

Svendsen, J., R. Sætre and M. Mork, 1991: Features of the northern North Sea circulation. Continental Shelf Res., **11**, 493–508.

Turrell, W.R., E.W. Henderson and G. Slesser, 1990: Residual transport within the Fair Isle Current observed during the Autumn Circulation Experiment (ACE). Continental Shelf Res., **10**, 521–543.

Turrell, W.R., 1992a: New hypotheses concerning the circulation of the northern North Sea and its relations to North Seafish stock recruitment. ICES J. mar. Sci., **49**, 107–129.

Turrell, W.R., 1992b: The East Shetland Atlantic Inflow. ICES mar. Sci. Symp., **195**, 127–143.

Submitted: July 23, 1993
Accepted: February 15, 1994

Authors' address:

Holger Klein
Wolfgang Lange
Dr. Ekkehard Mittelstaedt
Bundesamt für Seeschiffahrt und Hydrographie
Postfach 30 12 20
20305 Hamburg